Postprint of: Grabowska K., Szczuko P., Ship resistance prediction with Artificial Neural Networks, Signal Processing: Algorithms, Architectures, Arrangements, and Applications (SPA), Poznan (2015), pp. 168-173, doi: 10.1109/SPA.2015.7365154

Ship Resistance Prediction with Artificial Neural Networks

K. Grabowska, P. Szczuko
Faculty of Electronics, Telecommunications, and Informatics, Gdańsk University of Technology
Narutowicza 11/12, Gdańsk, PL80233, POLAND

***Abstract-* The paper is dedicated to a new method of ship's resistance prediction using Artificial Neural Network (ANN). In the initial stage selected ships parameters are prepared to be used as a training and validation sets. Next step is to verify several network structures and to determine parameters with the highest influence on the result resistance. Finally, other parameters expected to impact the resistance are proposed. The research utilizes parameters of 7 already built off-shore vessels, with model parameters available as a result of tests conducted on European towing tanks. Thus, the reference is used to assess ship resistance prediction with the artificial neural network approach.**

I. Introduction

Prediction of resistance of the ship at the initial design stage is of a great value for evaluating the ship's performance and for estimating the required propulsive power. The resistance and the total propulsive efficiency have to be determined with the highest possible accuracy. Essential inputs include the basic hull dimensions and the boat velocity expressed indirectly as a Froude number, expressing the flow inertia, i.e. speed–length ratio [17].

The resistance is important for ship owners and customers to reduce fuel consumption, and minimize the cost of model tests. In this study the main focus is on off-shore vessels due to the rising interest of the industry, and growing demands. Such ships are highly technologically advanced and last decades indicate great competition in this field. Trying to find more accurate and more up-to date methods for ship resistance estimation, an artificial neural network (Alyuda NeuroIntelligence) will be used [1], offering proven techniques for network design and optimization, a variety of training algorithms, including back propagation, conjugate gradient descent, Quasi-Newton and Levenberg-Marquardt methods.

II. Ship Resistance Prediction

Our work involves four types of off-shore vessels (Platform Supply Vessel (PSV), Anchor Handling Tug Supply Vessel (AHTS), Off-shore Construction Vessel (OCV), Seismic Support Vessel (SSV)). 19 parameters are available, and the most decisive were used for the ANN training.

Ship resistance is a result of two factors: main one, well defined and studied friction resistance, and pressure (residual) resistance. In accordance with International Towing Tank Conference Model-Ship Correlation Line [9] the C_F is defined by:

$$C_F = \frac{0.075}{(\log_{10} R_n - 2)^2} \quad (1)$$

where:

C_F – friction resistance coefficient, depends only on the Reynolds number.

R_n – Reynolds number:

$$R_n = \frac{v \cdot L_{WL}}{\upsilon} [-] \quad (2)$$

where:

v – vessel speed, relative flow velocity between the ship and the sea [m/s],

L_{WL} – length of waterline of ship [m],

υ – kinematic viscosity [m^2/s].

Thus, the total resistance coefficient C_T of a ship can be described as:

$$C_T(R_n,F_n)=C_F(R_n)+C_r(F_n) \quad (3)$$

where:

C_r – pressure (residual) resistance coefficient, depends on the Froude number,

F_n – Froude number:

$$F_n = \frac{v}{\sqrt{g \cdot L_{WL}}} [-] \quad (4)$$

and g – gravity of Earth [m/s^2].

Due to the precise and widely accepted definition of C_F (1), only the residual resistance coefficient as a function of Froude number $Cr(F_n)$ was estimated by the ANN in our work. From the model tests the C_r is available for a significant number of data points, and can be compared with the ANN result.

To find the optimum neural network configuration a random sample of the population was performed and independent data sets were created: a training set, a validation set, and a test set. For available 89 records data partition was established (Table I).

TABLE I
DATA PARTITION

Partition sets using	No. records	Percentage
Total	89	100%
Training set	61	68.54%
Validation set	14	15.73%
Test set	14	15.73%

A. Application of Artificial Neural Networks

ANN comprises a set of interconnected "artificial neurons", being a computational model inspired by natural neurons. Neurons receive signals through synapses, usually carrying encoded numeric data. When received signals are strong enough (surpass a certain threshold), the neuron is activated and emits an output signal through the axon. This signal might be sent to another synapse and might activate other neurons [16]. The artificial neuron model is highly abstract, consists inputs (synapses), multiplied by weights (strength of respective signals), and then transformed by a function determining the neuron activation. ANNs combine artificial neurons in order to process information.

ANN must be developed with a step-by-step procedure of adjusting weights, the process known as a training/learning rule. The input/output training data is fundamental for these networks as it conveys the information which is necessary to discover the optimal network state. Since the first neural model by McCulloch and Pitts (1943) there have been developed hundreds of different models considered as ANNs, differing in functions, accepted values, topology, and learning algorithms. ANNs were also used for creating an approximation model to an unknown non-linear function describing dependency between object (ship) parameters and result feature (resistance).

B. Ship Resistance Calculation Methods

Numerous tests conducted by every manufacturer, employing physical model of the ship indicate that numerical descriptions can't replace the experimental studies because of general divergences in the results (not necessarily high). On one hand the model test is an expensive procedure, providing precise results, but always subjectively interpreted by the researcher, and biased by his knowledge. On the other hand, prediction by numerical method gives rough estimation – proof of concept at the investment stage.

Widely known methods of ship resistance and propulsion model, such as Holtrop-Mennen [11][12] and its implementation as ANN [13], and Hollenbach [10] are shortly presented below. It is worth noting the Holtrop and Mennen's study performed 31 years ago haven't distinguished off-shore vessels yet, therefore the Authors' goal is to validate similar approaches for this new type of ships.

The **Holtrop-Mennen method** is used at the design stage for estimating ships resistances: $1+k$ expressing the form factor, and C_W – the wave's coefficient. A statistical evaluation of model test results was performed for data of Netherlands Ship Model Basin, by applying multiple regression analysis to each component for 1707 resistance measurements results, of 147 ship models, and 82 trial measurements made on board 46 real ships, resulting in R^2=0.636 for the form factor, and R^2=0.886 for the wave's coefficient. The method seems to track the experimental measurements approximately well, and the R^2 values are acceptable [11][12]. R^2 is coefficient of determination, expressing a degree of fitness between model and data.

Ortigosa et al. [13] presented an ANN predicting the same ship's parameters. Results shown suitability of applying the ANN, encouraging further research. A multilayer perceptron (MLP) with a sigmoid hidden layer and two linear outputs was used. Selected training algorithm was a quasi-Newton method with Broyden–Fletcher–Goldfarb–Shanno algorithm (BGFS) update [6] and Brent optimization [3][4]. This network was trained with generated data and experimental data to provide an estimation of the empirical model of output ($1+k$ and C_W) as functions of hull geometry coefficients and the Froude number, thus comprising 5 inputs (C_p, C_{stem}, L/B, B/T, and F_n).

The output values were calculated by Holtrop and Mennen's method for all possible combinations of input variables, thus forming the training data. The 20,664 generated cases were divided into a training (82%) and a validation (18%) subsets. Different numbers of neurons in the hidden layer were tested, and the network architecture providing best generalization properties for the validation data set was adopted. The result neural network was a 5:9:2 MLP, tested against experimental data of Beaver et al. [2], ITTC-Quality Manual [8], in order to assess the network performance and compare with Holtrop and Mennen's method. The linear regression yielded R^2=0.950 for the form factor, and R^2=0.998 for the wave's coefficient.

The ANN proposed by Ortigosa [13] improved the prediction over the entire range of data, comparing to Holtrop-Mennen approach.

The **Hollenbach method** [10] is based on regression analysis of 433 ships with varying main dimensions and forms coefficients. All data are from the Vienna Ship Model Basin, covering years 1980 to 1995. This analytical method is nowadays mostly used for calculating off-shore ship resistance, as it has proven the estimation results align with model test results. The regression is based on a length over surface parameter [16]. The method requires the aft body form and ship propulsion system to be specified.

III. Proposed ANN Configuration

Network architecture

Usually it is recommended to use only one hidden layer, as most of the problems can be solved by such an architecture. Input and output layers are determined based on the input data dimensionality and required output, thus the number of hidden layer neurons can be estimated as a geometric mean (5) [3]:

$$N_{hl} = \sqrt{N_{il} \cdot N_{ol}} \tag{5}$$

where:
N_{hl} - a number of neurons in a hidden layer,
N_{il} - a number of neurons in an input layer,
N_{ol} - a number of neurons in an output layer.

However, a performed automatic network architecture exploration revealed the N_{hl} = 24 gives the best accuracy. Therefore, several hidden layer configurations were tested, to investigate possible impact of architecture on the results.

Activation function

Empirically, a hyperbolic tangent activation function was chosen, characterized by a sigmoid shape curve, calculated using the formula: $F(x)=(e^x-e^{-x})/(e^x+e^{-x})$ (Fig. 1). Its output range is limited to <–1; 1>, therefore it suits the needs of modeling of also limited values.

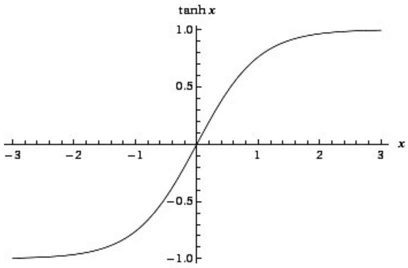

Fig. 1. Activation function hyperbolic tangent

Error function

Minimization of the error function is the main objective of the neural network training. The value of the error function is used to rate the quality of the neural network. Sum-of-Squared-Errors is the most common error function used for classification and regression problems. It is calculated as a sum of the squared differences between the actual value (target value) and observed neural network output:

$$SSE = \Sigma^{N}_{i=1}(x_i - \dot{x}_i)^2 \tag{6}$$

where:
x_i is the actual target value,
$\dot{x}_i$ is the estimated or forecasted value (output value).

Training algorithm

7 training algorithms were evaluated:

– Quick Propagation,
– Conjugate Gradient Descent,
– Quasi-Newton Programming,
– Limited Memory Quasi-Newton,
– Levenberg-Marquardt,
– Online Back Propagation,
– Batch Back Propagation.

A training algorithm best suiting the solved problem should be selected. Alyuda developers [1] suggest that for a network with a small number of weights (usually, up to 300), Levenberg-Marquardt algorithm is efficient, and it often performs considerably faster and finds better optima than other algorithms, however its memory requirements are proportional to squared number of weights, and it is specifically designed to minimize the SSE and cannot be used for other types of network error functions [15].

For networks with a moderate number of weights Quasi-Newton and Limited Memory Quasi-Newton [5] algorithms are efficient. But their memory requirements are also proportional to squared number of weights.

If the network has a large number of weights, it is recommend to use Conjugate Gradient Descent [7], as it has nearly the convergence speed of second-order methods, while avoiding the need to compute Hessian matrices. Its memory requirements are proportional to the number of weights.

For networks of any size also Incremental and Batch Back Propagation algorithms can be used. Back Propagation is the most popular algorithm for training of multi-layer perceptrons and is often used by researchers and practitioners. Its main drawbacks are: slow convergence, necessity to tune up the learning rate and momentum parameters, and high probability of training being caught in a local minima. Incremental Back Propagation can be efficient for large datasets if researcher properly selects the learning rate and momentum. It usually performs better than Batch Back Propagation [3].

IV. Experiments

For this research seven training algorithms were tested, and the following assumptions were made: network was retrained 3 times, stopping at iterations 10,000 and 100,000. Finally the network with best results was chosen. Results of the study are presented below in the Table II.

TABLE II
RESULTS OF THE TRAINING ALGORITHMS

Training algorithms	10,000 iterations			100,000 iterations		
	Corre-lation	R^2	AE	Corre-lation	R^2	AE
Batch Back Propagation	0.977	0.953	147.854	0.992	0.984	43.832
Conjugate Gradient Descent	0.994	0.988	27.141	0.999	0.998	41.599
Levenberg-Marquardt	0.997	0.994	42.235	0.996	0.994	42.236
Limited Memory Q Newton	0.988	0.975	28.292	0.999	0.998	21.413
Online Back Propagation	0.997	0.994	34.347	0.997	0.994	24.999
Quasi Newton	0.999	0.998	22.494	0.999	0.998	22.495
Quick propagation	0.999	0.997	21.770	0.998	0.998	16.737

where: AE – absolute error, R^2 – coefficient of determination

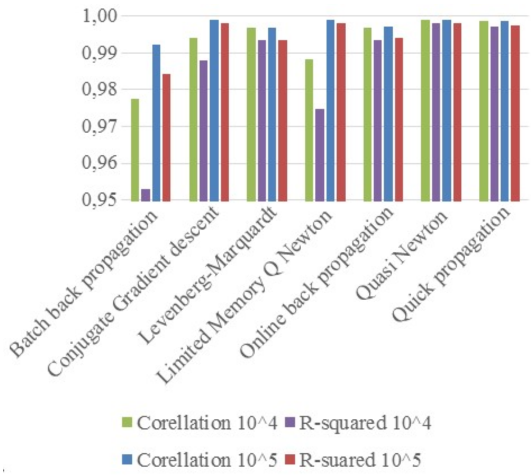

Fig. 2. Results of the training algorithms for available training algorithms and given number of iterations

For Levenberg-Marquardt algorithm, despite the set number of iterations, the training stopped much earlier, as it is sensitive to local minima. It changes network weights using a quadratic approximation of error surface. Such approximation can help finding a minimum quickly, nevertheless it increases the possibility of converging into a local minimum. For Quasi-Newton algorithm anomalies occurred and number of iterations had to be decreased.

Quick Propagation gives the most promising results for correlation between target and output values, R^2 and absolute validation error. Therefore further study will be conducted for this algorithm, and it is briefly described below.

Quick Propagation calculates the weights change Δw by using the parabolic function $f(x)=x^2$. Two error values are obtained by applying two weights, being points of a secant. Relating the secant to the function, its minimum can be found $f'(x) = 0$. The x-coordinate of the minimum point is a new weight value [14]. The slope in this particular point is calculated as:

$$S(t)=\frac{\partial E}{\partial w_i(t)} \tag{7}$$

Then, it can be assumed that:

$$\frac{\Delta w_i(t)}{\alpha}=\frac{\partial E}{\partial w_i(t)} \tag{8},$$

what results in:

$$S(t)=\frac{\partial E}{\partial w_i(t)}=\frac{\Delta w_i(t)}{\alpha} \tag{9},$$

and finally, a formula for Quick Propagation adjustments of the weights based on the previous (t-1)-th iteration:

$$\Delta w_i(t)=\frac{S(t)}{S(t-1)-S(t)}\cdot\Delta w_i(t-1) \tag{10}$$

For normal backpropagation it was:

$$\Delta w_i(t)=\alpha\cdot\frac{\partial E}{\partial w_i(t)} \tag{11}$$

where for equations (7–11):

w – weight,
E – error function,
t – time (training step),
α – learning rate.

To avoid too large changes during the training the maximum weight adjustment was finally limited by applying:

$$\Delta w_i(t)\le\mu\cdot\Delta w_i(t-1) \tag{12}$$

where: μ – maximal weight change factor.

Once the used algorithm was selected, the next step was to find best network architecture. For this purpose several cases were considered with 4, 6, 9, 12, 15, 18, and 24 neurons in a hidden layer. 24 neurons give the lowest absolute validation error (Fig. 3), therefore the network architecture 20-24-1 was used in the further study.

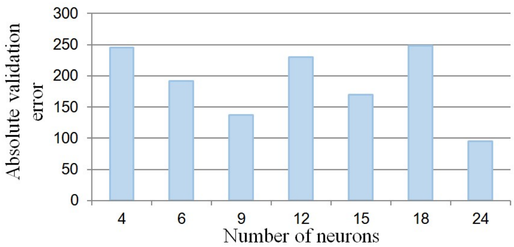

Fig. 3. Absolute validation error to number of neurons

The overall accuracy is presented in Fig. 4, as a scatter plot.

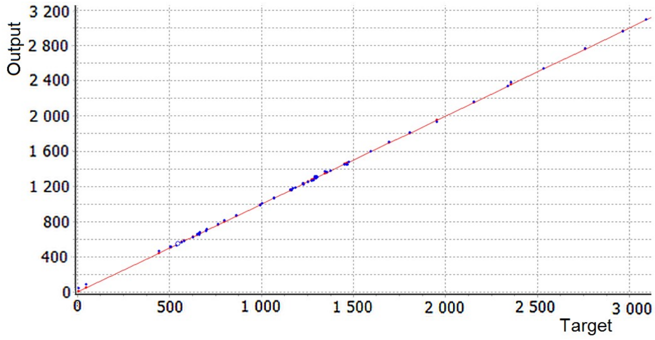

Fig. 4. Scatter plot, revealing strong correlation of obtained output and target values

Training summary is presented in Table III.

TABLE III
TRAINING SUMMARY OF NETWORK ARCHITECTURE 20-24-1

	Target	Output	AE	ARE
Mean	1273.64	1274.03	9.54	0.10
Std deviation	794.01	788.98	8.85	0.65
Min	7	42.36	0.013	0.00001
Max	4869	4823.56	45.44	5.05

where:

Target – the target value taken from input data file,
Output – the output produced by the network,
AE and *ARE* – absolute error and absolute relative error. The difference between the actual value of the target column and the corresponding network output.

As a sample results, two vessels, PSV no.6 and AHTS no. 79 are discussed here. Following values (Table IV) of the residual resistance coefficient were obtained.

TABLE IV
RESULTS OF RESIDUAL RESISTANCE COEFFICIENT FOR OFF-SHORE VESSELS

PSV no. 6			**AHTS no. 79**		
F_n [-]	C_r·10E-6 [-] Target	C_r·10E-6 [-] Output	F_n [-]	C_r·10E-6 [-] Target	C_r·10E-6 [-] Output
0.139	547	546	0.170	1411	1557
0.157	581	581	0.188	1451	1442
0.174	542	569	0.205	1538	1462
0.192	509	514	0.222	1695	1693
0.209	540	531	0.239	1954	1943
0.227	705	710	0.256	2358	2364
0.244	959	1074	0.273	2965	2959
0.262	1597	1596	0.290	3849	3652
0.279	2762	2762	-	-	-

where:

F_n – Froude number,
C_r – residual resistance coefficient.

The correspondence between actual and predicted values of C_r for selected two vessels is presented in Fig 5–6. The model is not able to correctly match target values for medium F_n in case of PSV6 and low and high F_n for AHTS79.

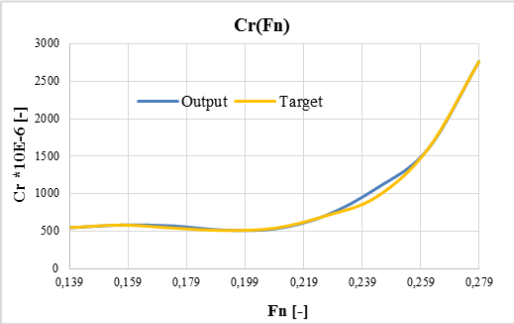

Fig. 5. Residual resistance coefficient as a function of Froude number, PSV no. 6

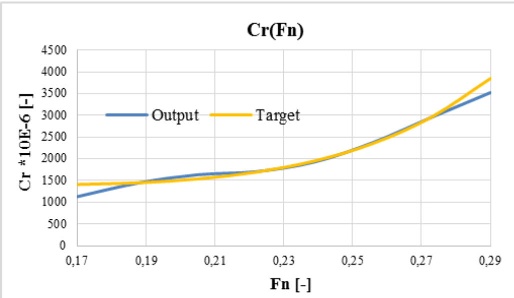

Fig. 6. Residual resistance coefficient as a function of Froude number, AHTS no. 79

V. Further Study – New Parameters Recommendation

Four additional parameters describing the shape of the bulb, and potentially influencing the residual resistance were proposed by the Authors. New parameters are (Fig. 7):

- Bulb bow cross-section on the forward perpendicular A_{BFP} [m^2]
- Bulb bow middle cross-section A_{BM} [m^2]
- Distance between forward perpendicular and the most forward point on the bulb bow L_B [m]
- Height of the bulb bow measured on the forward perpendicular H_B [m].

Instead of using absolute values, two ratios were derived: A_{BFP}/ A_{BM}, and L_B/H_B. Due to the software limitation of handling up to 20 input data, these coefficients had to replace inputs with the smallest level of importance, i.e. L_{CB} and L_{WL}.

TABLE V
PROPOSED PARAMETERS DESCRIBING BULB BOW

Lp.	Ship no.	Type of off-shore vessel	A_{BFP} [m^2]	A_{BM} [m^2]	A_{BFP}/ A_{BM} [-]	L_B [m]	H_B [m]	L_B/ H_B [-]
1	6	PSV	14.10	7.37	0.52	5.11	6.47	0.79
2	21	OCV	27.94	14.50	0.52	6.84	9.90	0.69
3	46	SSV	11.34	6.71	0.59	3.84	6.13	0.63
4	50	OCV	20.62	11.18	0.54	5.53	7.89	0.70
5	69	AHTS	23.42	13.53	0.58	5.00	7.96	0.63
6	72	OCV	26.34	13.41	0.51	6.45	9.11	0.71
7	79	AHTS	24.10	12.32	0.51	5.70	7.94	0.72

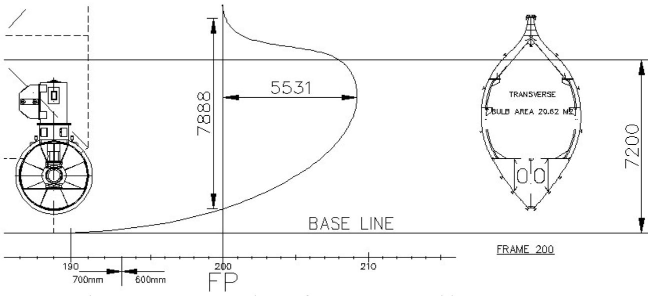

Fig. 7. Parameters values of L_B, H_B, A_{BFP}. Ship OCV no. 50

After retraining with new parameters, the accuracy of the neural network slightly increased. Therefore, it is recommended that proposed variables should be taken into account while calculating the residual resistance coefficient. Detailed results for selected off-shore vessels are presented in (Table VI).

TABLE VI
RESULTS OF RESIDUAL RESISTANCE COEFFICIENT FOR OFF-SHORE VESSELS

PSV no. 6			AHTS no. 79		
F_n [-]	C_r·10E-6 [-] Target	C_r·10E-6 [-] Output	F_n [-]	C_r·10E-6 [-] Target	C_r·10E-6 [-] Output
0.139	547	403.844455	0.170	1411	1410.77756
0.157	581	580.332409	0.188	1451	1444.517449
0.174	542	550.116745	0.205	1538	1536.88167
0.192	509	495.809705	0.222	1695	1695.663287
0.209	540	546.825623	0.239	1954	1952.705234
0.227	705	704.413058	0.256	2358	2412.467895
0.244	959	1004.604662	0.273	2965	2964.692068
0.262	1597	1595.903934	0.290	3849	3932.515262
0.279	2762	2761.925053	-	-	-

The correspondence between actual and predicted values of C_r with new parameters applied in the training phase, for selected two vessels is presented in Fig 8–9.

Comparing results of initial parameters set (Fig. 5–6) with accuracy for new parameters including bulb bow geometry (Fig. 8–9) it can be noted an improvement was achieved, and SSE_{init}=80.266, SSE_{new}=32.849, MSE_{init}=4.722, and MSE_{new}=1.932. The improved model matches target values better, especially in case of AHTS79.

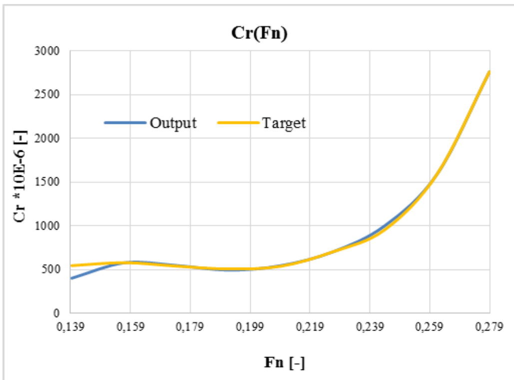

Fig. 8. Residual resistance coefficient as a function of Froude number, PSV no. 6

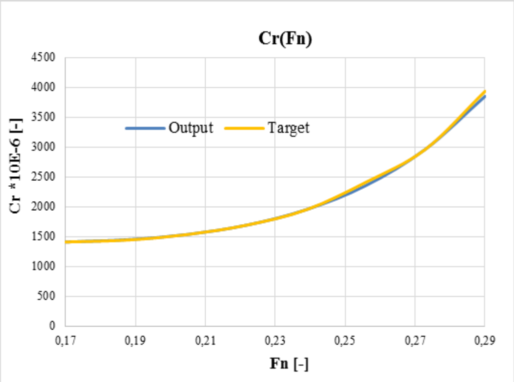

Fig. 9. Residual resistance coefficient as a function of Froude number, AHTS no. 79

VI. Conclusions

Neural networks had proven to be a very useful tool for data modeling tasks. Numerical descriptions of ship performances, namely Holtrop-Mennen and Hollenbach methods are widely used in a maritime world. Model tests play a very important role in the initial ship design. Results from the numerical methods for off-shore vessels often need to be tuned based on the similar vessels from a preceding model test. It can be expected that in the future it will be possible for numerical description to replace the model tests. The next acknowledged method of developing a numerical description of ship performance, using basic hull dimensions, might be Artificial Neural Network.

The proposed and trained network shown satisfactory accuracy compared with the results from the model tests. Nevertheless, the architecture might be improved and further study of this approach should be undertaken.

Proposed new parameters improved the accuracy of obtained results, and involving other parameters in future studies is advised.

References

1. *Alyuda Neurointelligence 2.2 (577) Manual.* Alyuda Research 2001-2005.
2. Beaver W., Day W, Chwg-Wen L *Resistance and propulsion characteristics of the MarC Guardian tanker design*. MARINEX International, Advanced double-hull Technical Symposium. 1994
3. Bishop C.M., *Neural Networks for Pattern Recognition*. Oxford University Press 1995.
4. Brent R.P. *Algorithms for Minimization without Derivatives*, Englewood Cliffs, NJ: Prentice-Hall, 1973
5. Byrd RH, Lu P; Nocedal J, Zhu C, *A Limited Memory Algorithm for Bound Constrained Optimization*. SIAM Journal on Scientific and Statistical Computing, Vol. 16, No. 5, pp. 1190–1208, 1995
6. Dennis, J.E., and R.B. Schnabel, *Numerical Methods for Unconstrained* Optimization *and Nonlinear Equations*, Englewood Cliffs, NJ: Prentice-Hall, 1983.
7. Hazewinkel M, *Conjugate gradients, method of*, Encyclopedia of Mathematics, Springer, 2001
8. ITTC – *Quality Manual. Resistance Uncertainly Analysis, Example for Resistace test.* 22nd International Towing Tank Conf., 1999
9. ITTC – *Recommended Procedures. Performance, Propulsion 1978 ITTC Performance Prediction Method*. International Towing Tank Conference 1999.
10. Hollenbach K.U., *Estimating resistance and propulsion for single screw and twin screw ships*, Ship technology research, 1998
11. Holtrop J., Mennen G.G.J., *An approximate power prediction method*. International Shipbuilding Progress 29, p. 166 – 170, 1978.
12. Mennen G.G.J., Holtrop J., *A statistical re-analysis of resistance and propulsion data*, ISP, Vol. 31, No. 363, 1984.
13. Ortigosa I., Lopez R., Garcia J., *Prediction of total resistance's coefficients using neural networks,* 2009.
14. Priddy K.L., Keller P.E., *Artificial Neural Networks: an introduction.* Bellingham, Washington 2005.
15. Pujol J, *The solution of nonlinear inverse problems and the Levenberg-Marquardt method*, Geophysics (SEG), Vol. 72, No. 4, 2007
16. Rojas, R. *Neural Networks: A Systematic Introduction*. Springer, Berlin 1996
17. White F.M. , *Fluid Mechanics*, p. 294, McGraw-Hill, 1999

APPENDIX 1: Off-shore vessels types


a)


b)


c)

d)

Contours of off-shore vessels: a) Platform Supply Vessel (PSV), b) Anchor Handling Tug Supply Vessel (AHTS), c) Off-shore Construction Vessel (OCV), d) Seismic Support Vessel (SSV).

Sources:
PSV (https://commons.wikimedia.org/wiki/File:PSV_Skandi_Texel.jpg)
AHTS (https://commons.wikimedia.org/wiki/File:Normand_Master.jpg)
OCV (https://commons.wikimedia.org/wiki/File:The_North_Sea_Giant_in_Bangor_Bay_01.jpg)
SSV (https://commons.wikimedia.org/wiki/File:Polarcus_Amani.jpg)